JCBPS; Section D; February 2026 to April 2026, Vol. 16, No. 2; 287-296. E- ISSN: 2249 –1929
[DOI: 10.24214/jcbps.D.16.2.28796.]

Journal of Chemical, Biological and Physical Sciences

An International Peer Review E-3 Journal of Sciences

International scientific indexing (ISI) Impact Factor (2025-2026) 03.616

*Available online at*www.jcbsc.org

Section D: Environmental Sciences

CODEN (USA): JCBPAT Research Article

Modelling the impact of flow velocities on the development of aquatic plants in the Bango Reserve

Mahecor DIOUF[1], Dior DIALLO[1], Mamadou Salif DIALLO[2], Abdou Rahmane SONKO[1], Papa Saer WADE[1], Boubacar CISSE[3], El Hadji Bamba DIAW[4]

[1]National School of Agriculture (ENSA)

[2]Alioune Diop University of Bambey (UADB)

[3]Office of Lakes and Rivers (OLAC)

[4]International Institute for Water and Environmental Engineering-2iE

Received: 03 January 2026**; Revised:** 31 January 2026**; Accepted:** 12 February 2026

Abstract: The Bango water reserve is subject to issues of aquatic plant proliferation, suspended matter deposits, and the impacts of climate change. This study aims to identify the impact of flow velocity on the development of aquatic plants in the Bango reserve. The methodological approach primarily relied on the development of a numerical model to understand the hydraulic behaviour of the reserve in the presence of invasive plants. The analysis of the impact of climate change in this study considered the withdrawals due to this factor for the years 2050 and 2100. The results of climate projections from the Senegal Geoportal under scenarios RCP 2.6, RCP 4.5, and RCP 8.5 were used to estimate future potential evapotranspiration and corresponding withdrawals. The results of direct withdrawals by potential evapotranspiration indicated respective increases of 21% and 32%, corresponding to additional evaporation demands of 3,543,301 m^3/year and 5,321,154 m^3/year projected for 2050 and 2100. A superimposition of the land use layer of the reserve and the velocity contour lines shows an absence of aquatic plants in areas where the flow velocity exceeds 0.014 m/s. The results of simulations conducted with the HEC-RAS software showed that increasing the flow rate to 11 m^3/s would limit the development of Typha over an area of approximately 103 hectares if withdrawals are not taken into account. However, if withdrawals are considered, managing with a flow rate of 11 m³/s is a feasible solution, but a reduction of 5.3% in impacted areas is noted compared to the initial scenario. For future withdrawals, management with respective flows of 22 m³/s and 35 m³/s could be considered, with respective reductions in impacted areas of 6% and 7% compared to the initial scenarios.

Keywords: Bango reserve, aquatic plants, flow velocities, climate change, Typha.

1.INTRODUCTION

The development of aquatic plants has been a major problem in the Senegal River delta for several decades. The development of irrigated perimeters necessitated the establishment of hydraulic structures and axes in the area. This has consequently created an environment conducive to the development of aquatic plants. The Bango reserve, whose quantitative and qualitative water monitoring is managed by the Office of Lakes and Watercourses (OLAC), like all water bodies in the delta, is subject to water quality issues due to the development of aquatic plants, suspended matter deposits, and the impacts of climate change. Indeed, the rotting of Typha stems on site deteriorates water quality, rendering it unusable for drinking by local populations (UNDP, 1999). It is within this vast perspective that this research article on modeling the impact of flow velocities on the distribution of aquatic plants in the Bango reserve under various scenarios is situated.

2.MATERIALS AND APPARATUS

2.1. Presentation of the study area: The Bango reserve is identified at the downstream section of the Gorom-Lampsar-Djeuss system, which consists of a series of secondary branches of the Senegal River. It is bounded:

- To the north by the Bango dike where the Bango structure is located;
- To the east by the departmental road D401B connecting Saint-Louis to Diama, where the Mboubène structure is located;
- To the south by national road No. 2;
- To the west by the villages of Sanar and Bango.

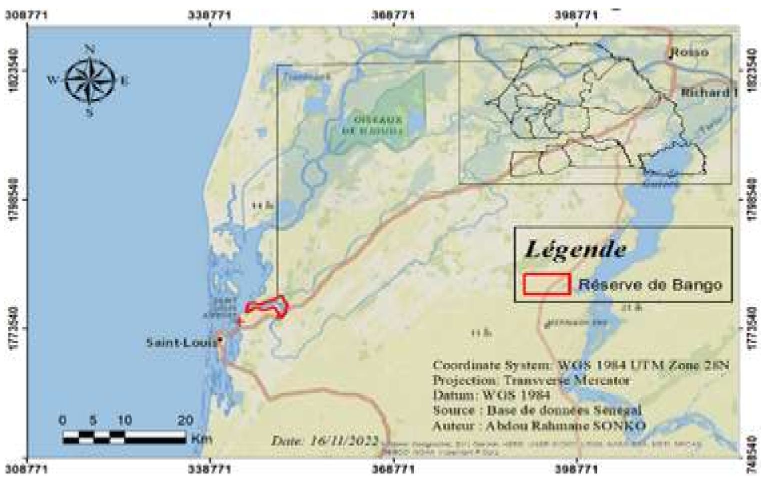

Figure 1: Position of Bango reserve

The map in **Figure 1** shows the position of the Bango reserve within the lower delta system and Senegal in general.

Data Used: The data used in this study includes:

- Topographic and bathymetric data and withdrawals from the Bango reserve and the downstream Lampsar collected from the databases of SAED and OLAC;
- Limnometric data collected within OLAC;
- Climate data from the Saint Louis meteorological station;
- Population data of Saint Louis and growth rates collected from the ANSD website; and;
- Climate change projection results from the Senegal
- Geoportal: http://geoportail.anacim.sn:8000/climap/proj/ were utilized in this study. This tool provides access to projections of temperatures, rainfall, and agricultural yields from 29 MCC under three scenarios:
  - RCP 2.6: low emissions scenario (optimistic);
  - RCP 4.5: medium emissions scenario;
  - RCP 8.5: high emissions scenario (pessimistic).

Data Procession : Data processing required the use of several tools (software) including:

- Autocad/Covadis for processing topographic and bathymetric databases to define the geometry of the hydro system that constitutes the Bango reserve;
- ArcGIS for creating the digital terrain model (DTM) based on topographic and bathymetric data, as well as determining morphometric parameters and mapping the reserve;
- HEC-RAS for constructing the free surface flow model and observing the results of various simulations;
- INSTAT+ applying the PENMAN formula to calculate ETP, and ;
- Microsoft Office for data processing, calculations, and graph representation.

Equipment: The following equipment was used for field data collection:

An ADCP flowmeter used to measure average flow velocity at the Ndiawdoune and Mboubène structures. It automatically configures through wireless communication via Bluetooth to a laptop. Using the Win River software, all relevant information (flow profile, current flow rate, velocity, etc.) is clearly provided to the user.

A GPS for collecting topographic coordinates and a computer for data processing.

Figure 2 : ADCP flowmete GPS GARMIN Computer

DOI:10.24214/jcbps.D.16.2.28796.]

2.2. Construction of the Free Surface Flow Model with HEC-RAS and Calibration: The HEC-RAS software is developed and distributed free of charge by the Hydrologic Engineering Center of the US Army Corps of Engineers. HEC-RAS is a simulation software for flows in rivers and channels. Version 6.3.1 of the HEC-RAS software was used for constructing the free surface flow model. However, it requires a number of data including the Digital Terrain Model (DTM), flow data, water height data, etc. The calibration of the model in HEC-RAS essentially involves determining the correct Manning coefficients to reproduce the observed results in the field, as these are the parameters most sensitive to observed flow rates and water levels. However, lacking sufficient observed data for comparison between observed and simulated values, the instantaneous flow measurements taken at the Ndiawdoune and Mboubène structures, as well as the observed water heights at the Bango structure, were used as reference values for calibration.

2.3. Calculation of Flood Propagation in Non-Permanent Flow Regime :T he HEC-RAS software operates according to the Saint-Venant equations, which describe quasi-one-dimensional flow in a channel. To do this, it uses two conservation equations:

- the principle of mass conservation and the principle of momentum conservation, both expressed in the form of differential equations. The principle of mass conservation (or continuity equation) is given by the equation below:

$$\frac{\partial A}{\partial t} + \frac{\partial Q}{\partial x} - ql = 0$$

A = Control area [m²];

Q(x, t) = Flow rate [m³/s];

and ql = lateral flow per unit length [m³/m.s].

- The principle of momentum conservation is given by the equation below: Le principe de conservation de la quantité de mouvement à partir de l'équation ci-dessous:

$$\frac{\partial Q}{\partial t} + \frac{\partial QV}{\partial x} + gA(\frac{\partial z}{\partial x} + Sf) = 0$$

A = Control area [m²],

Q(x, t) = Flow rate [m³/s],

V = Velocity [m/s],

Sf = friction slope (calculated according to the Manning equation).

2.4. Definition of hydrosystem geometry: The hydrosystem geometry defines the geometric characteristics of the modeled system, such as the tree diagram of the watercourse, junctions, bank lines, high-water lines (limit of the model's zone of influence), cross-sections, Manning's roughness coefficients on each cross-section portion, etc.

This step was carried out using the RAS mapper and on the basis of the DTM digital terrain model generated with Arc GIS software from topographic and bathymetric surveys of the reserve.

The figure below shows the result of overlaying the DTM with the geometry components

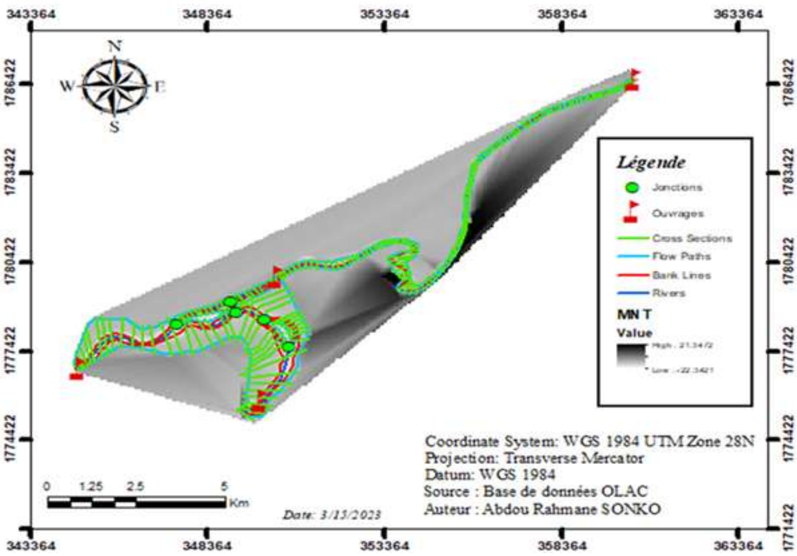

Figure 3: Components of hydro system geometry

Hydraulic structures in the reservoir can strongly influence water levels, which is why it is important to take them into account in the model. The structures are modeled using the geometry editing window, which involves specifying their position, the dimensions of the invert, the crest of the dike, the structure, the slope of the embankments and other characteristics such as the type of structure, the number of gates, etc.

3.RESULTS AND DISCUSSION

3.1. Analysis of Withdrawal Results: The analysis of the withdrawal balance results at the Bango reserve shows that evaporation losses represent 49%. This allows us to assert that climate has a significant impact on the reserve's capacity. Additionally, annual needs are estimated at 34,100,587.31 m^3/year. Thus, to meet these needs, a continuous inflow of 1.08 m^3/s is necessary. The tables below provide the results of the evolution of various withdrawals.

Table 1: Evolution of Withdrawals for 2100

Population of Saint Louis (hbts)	Projected population of Saint Louis in 2050 (hbts)	Projected population of Saint Louis in 2100 (hbts)	Need 2050 (m^3/jr)	Need 2100 (m^3/jr)
216818	547160	2134614	48150,11	187846,04

Livestock (cattle+small ruminants	Projected population of Saint Louis in 2050 (hbts)	Projected population of Saint Louis in 2100 (hbts)	Need 2050 (m^3/jr)	Need 2100 (m^3/jr)
1000	3262	14300	97,86	429,01
350	1142	5005	5,71	25,03
Growth rate	3%	Total (m^3/jr)	103,57	454,04

According to projections, an increase in evaporation of 21% is noted for the three scenarios by 2050 and 32% by 2100, corresponding to additional volumes of 3,543,301 m^3 and 5,321,154 m^3, respectively. Concerning total withdrawals, they correspond to 48,361,367 m^3/year by 2050 and 101,788,139 m^3/year by 2100 if the most pessimistic scenario is considered. Furthermore, to meet the

DOI:10.24214/jcbps.D.16.2.28796.]

needs by 2050 and 2100, respective flows of 1.53 m³/s and 3.23 m³/s will need to be admitted at the Mboubène structure, the main entry of the Bango reserve.

3.2. Analysis of initial velocity distribution: The results of the transient HEC-RAS simulation were used to visualize the horizontal velocity distribution. By importing the Velocity shapefile into Arc GIS, we were able to generate the velocity contours and see their distribution over the entire reserve

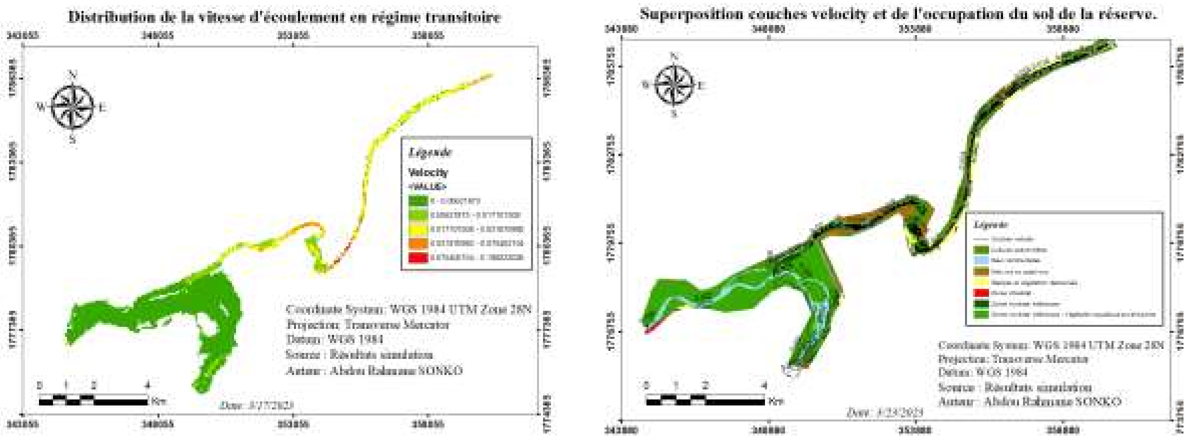

Figure 4 : Distribution de la vitesse d'écoulement en régime transitoire ** Superposition couches Velocity et de l'occupation de la réserve

Analysis of flow velocities shows that over the whole reserve, velocities are low, varying between 0 and 0.198 m/s. This is due to the fact that the Bango reserve is a shallow reservoir. The absence of inlets upstream and downstream, the constraints of water heights to be respected downstream, a slope, following the example of the river delta, extremely low, of the order of 0.006‰ at the time of medium water to 0.01‰ by high flood which justifies the very low velocity ranges despite the flows and conditions imposed.

3.3. Horizontal velocity distribution in a section: An overlay of the Velocity layer with that of the reserve's land use, highlights the distribution of flow velocity according to the different land use classes

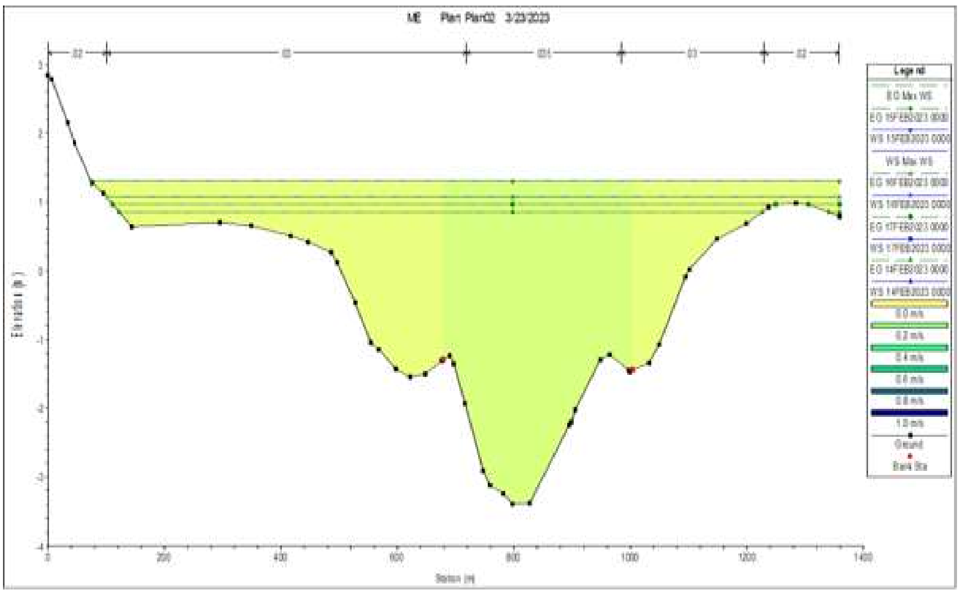

Figure 5: Horizontal velocity distribution in a section

DOI:10.24214/jcbps.D.16.2.28796.]

Analysis of the figure 5 shows the absence of Typha in areas where flow velocities exceed 0.014 m/s. The model was then used to carry out simulations to optimize the flow rate that needs to be adjusted upstream in order to maintain a range of velocities that would not encourage Typha development downstream, taking into account the different water withdrawals (current, 2050 and 2100). To achieve this, new boundary conditions are set, essentially concerning the number of gates open and their opening heights.Five flow scenarios were tested in order to visualize their impact, and that of sampling, on horizontal velocity distribution.Flow velocity must be greater than or equal to 0.014 m/s to prevent the development of aquatic plants, based on the analysis of velocity distribution in the initial state. The imposed upstream flows selected are as follows: 11m3/s, 15m3/s, 22m3/s, 35m3/s, 73m3/s. The boundary conditions defined are listed in the table below.

Table 2: Limit conditions

Site/position	Number of valves	Number of open valves	Number of closed valves	Opening height
Mboubène	2	2	0	2.15 m
Ndiawdoune	7	3	4	1.5 m
Bango	6	6	0	1.5 m

Horizon	Q (m^3/s)	Q (m^3/h)	Number of pumps
Current levy	1,08	3893	10
Withdrawal in 2050	1,53	5521	14
Withdrawal in 2100	3,23	11620	30

After the various simulations, the results were displayed by mapping the velocity values. The analysis consists of visualizing the effect of increased flow on the displacement of the NC 0.014m/s on either side of its initial position, and digitizing the corresponding areas. By superimposing the velocity curves on the land-use map, we were able to estimate the width and surface area gained for each flow profile.

The analysis of the results of the various simulations with sampling was based on the results obtained from the initial scenarios, i.e. without any consideration of sampling, and compared with the NC 0.014m/s obtained.As a reminder, current abstractions are estimated at 1.08 m3/s. Figure 27 shows the contour lines for the various scenarios simulated with current abstractions, compared with those obtained if abstractions are not taken into account (reference CN 0.014m/s).

Analysis of the results for simulations of various scenarios reveals that increasing the upstream flow reduces the area covered by invasive aquatic vegetation. This suggests that increased flow affects the growth of aquatic vegetation by decreasing the occupied area. For a given section, an increase in water flow increases the speed, which can delay vegetation growth by preventing the sedimentation of suspended particles and thus hindering the establishment of seeds or propagules.

However, taking into account water abstractions showed that, for the same flow scenarios, abstractions lead to reductions in sections and subsequently in impacted areas. Indeed, current water abstractions have revealed a reduction in affected areas of up to **9%**. By 2050, a reduction of up to **25%** is projected. By 2100, this reduction could reach up to **77%**. This can be attributed to the fact that water abstractions lead to a decrease in the flow rate, which consequently reduces the impacted areas, especially as larger abstractions are made.Furthermore, the analysis showed that across all abstraction scenarios (current, 2050, and 2100), an increase in the flow rate up to **73 m3/s** would mitigate the impact of abstractions on the reduction of affected areas.

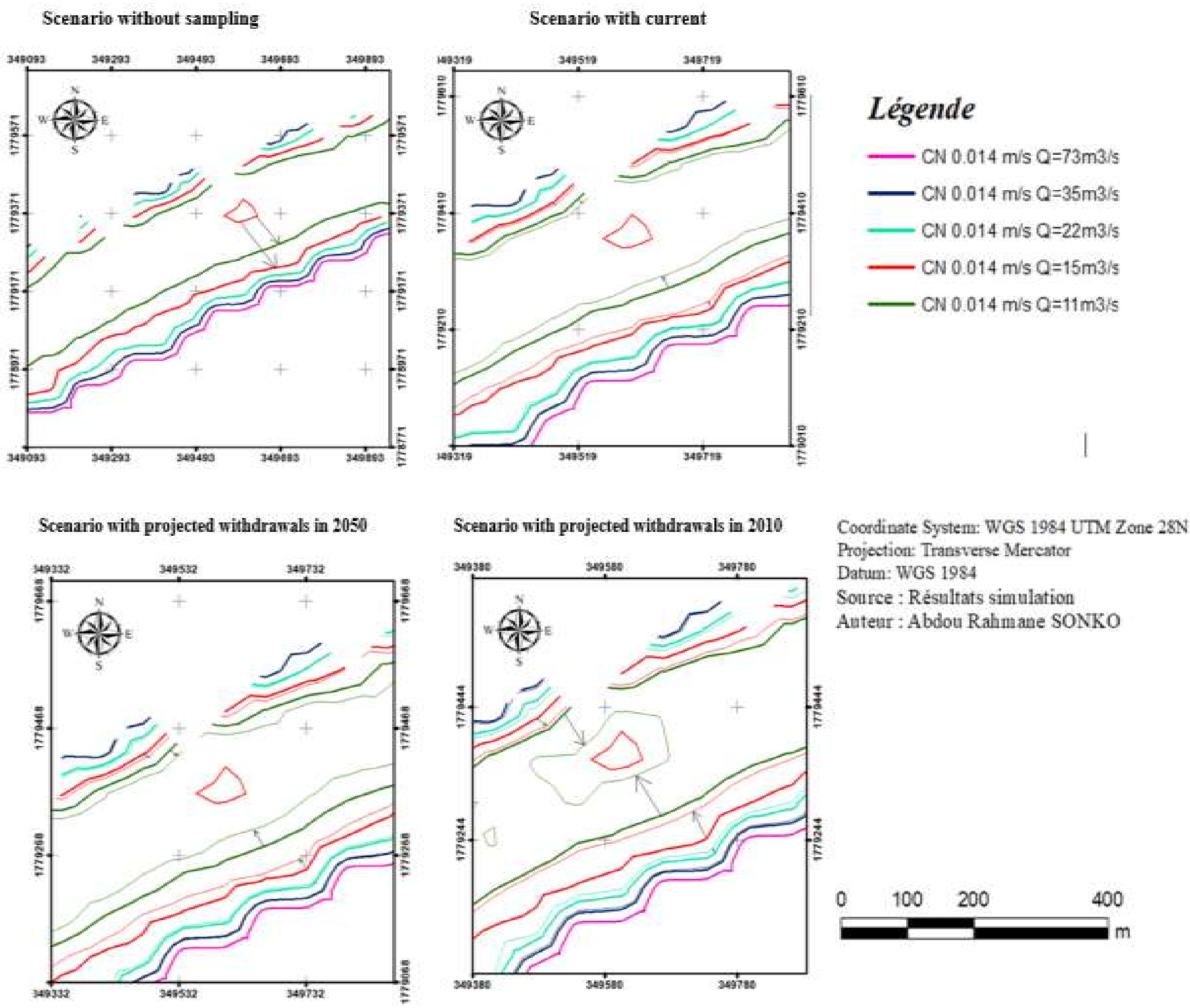

Figure 6 : Contours of the 0.014m/s speed for the different scenarios

Table 3: Summary of simulation results

Scenarios tested	**Level curve displacement 0.014 m/s (m)**	**Impacted areas (ha)**	**Level curve displacement differences 0.014 m/s (m)**	**Difference impacted areas (ha)**	**Variation (%)**
Q=11m^3/s	59	77	30	26	25
Q=15m^3/s	130	113	12	13	10
Q=22m^3/s	174	162	3	9	5
Q=35m^3/s	193	192	3	10	5
Q=73m^3/s	214	273	1,1	6	2

Nevertheless, current abstraction levels do not substantially lower the areas impacted by the increase in upstream flow, even for a flow rate of **11 m3/s**. By 2050, an upstream flow rate of **22 m3/s** could help limit the reduction in the impacted areas. By 2100, a flow rate of **35 m3/s** would similarly help mitigate reductions caused by increased flow.

CONCLUSION

The results of climate change projections from Senegal's Geoportal under RCP 2.6, RCP 4.5, and RCP 8.5 scenarios were utilized in this study to estimate future ETPs (Evapotranspirations) and the corresponding abstractions. The study revealed that direct abstractions through evapotranspirations represent the largest share of water taken from the reserve, and that climate change significantly impacts the water availability in the reserve. Specifically, projected increases of **21%** and **32%** are foreseen by 2050 and 2100, respectively.

Furthermore, simulation results under HEC-RAS with various flow scenarios indicated that increasing flow up to **11 m3/s** could limit the development of aquatic vegetation in much of the reserve, with a noticeable vegetation clearing of **103 hectares**.However, results also showed that considering current abstractions, maintaining a flow of **11 m3/s** could be feasible but would reduce the affected area by approximately **5%**, which translates to **5 hectares**.

Regarding abstractions in 2050 and 2100, maintaining respective flow rates of **22 m3/s** and **35 m3/s** could be envisaged. This would limit the impact of abstractions on area reductions by approximately **5%** in 2050 and **7%** in 2100, corresponding to **9 hectares** and **14 hectares**, respectively.

REFERENCES

1. Anne CALESTREME. Invasion of *Typha australis* in the Senegal River Basin, 2002, p 31.
2. Bayol B. Computer system for assisting mathematical modeling based on a dedicated programming language for stochastic discrete dynamic systems, 2016.
3. C. Hermel, J Chorda, M.M. Maubourguet, D. Dartus. Dynamic flood slowdown: Evaluation of the hydraulic impact of current-breaking hedges, 2010, p 39.
4. G. Degoutte, Course on hydraulics, dynamics, and morphology. Paris: National School of Rural Water and Forestry Engineering, 2006.
5. A.Galema, Vegetation resistance: Evaluation of vegetation resistance descriptors for flood management. Master's project, Faculty of Engineering and Technology, University of Twente, 2009.
6. M.A.Golzar, brief review of pond residence time studies, in: The Annual Postgraduate Research Student Conference-2015, 2015.
7. HYDRO-BLOG. (2019, May 26). HEC-RAS: Software for river modeling (free). *Hydroblog*. Available at: [Hydro-blog](https://hydro-blog.com/hec-ras/)
8. Z.Sirabahenda, Numerical modeling of suspended sediment transport in a river under development: Case of the Rivière-aux-Sables in Quebec, 2012, 105p.
9. J.D.Shucksmith, J.B.Boxall, I. Guymer, Effects of emergent and submerged natural vegetation on longitudinal mixing in open channel flow. Water Resour. Res, 2010, 46p.

10. A.Tsavdaris, S. Mitchell, B.J. Williams, Use of CFD to model emergent vegetation in detention ponds. ARPN J Eng Appl Sci 8, 2013, pp 495–503.

11. U.S. Army Corps of Engineers. HEC-RAS (Version 4.1) [Hydraulic Reference Manual]. Davis, CA: Hydrologic Engineering Center, U.S. Army Corps of Engineers, 2008.

*** Corresponding author: Mahecor DIOUF;**

[1]National School of Agriculture (ENSA);

Online publication Date: 13.02.2026